Applications of ultrasound imaging system for measuring water-sand parameters during sediment transport process in hydraulic model experiments

Xianjian Zou, Chuanying Wang, Huan Song, Zengqiang Han, Zhimin Ma and Weinbin Hu

ABSTRACT

Moving particles and the topographic bed under muddy water or in sediment-laden flow are often clouded by suspended sediments, making it hard to detect or analyze for visualization. This paper concerns applications of ultrasound imaging measurement method for the visual measurement of related water-sand parameters during sediment transport process in hydraulic model experiments. We use a B-mode ultrasound imaging system to measure the related parameters of suspended sediment concentration (SSC), underwater topographic riverbed, flow velocity and sediment incipient motion, conducted at a water channel. A comprehensive measuring system for the visualization of multiple water-sand parameters is established. Results show that the measurement and analysis of SSC and its space distribution, topography bedform, flow velocity and flow field, and sediment incipient velocity can be realized. Ultrasound imaging measurements of SSC and their space distribution can be shown in real time, and also dynamic monitoring and analysis of sediment incipient motion and topography bedform during the sediment transport process. This method realizes the experimental visualization of the topographic bed and sediment-laden flow. Application of an ultrasound imaging measurement system has promoted the development of sediment movement law research and related hydraulic model experiment measurement technique.

Key words | flow velocity, sediment incipient velocity, sediment transport process, suspended sediment concentration, topography bedform, ultrasound imaging measurement method

Xianjian Zou (corresponding author)
Chuanying Wang
Zengqiang Han
State Key Laboratory of Geo-mechanics and Geotechnical Engineering, Institute of Rock and Soil Mechanics,
Chinese Academy of Sciences,
Wuhan, Hubei 430071,
China
E-mail: *zouxianjian@whu.edu.cn*

Xianjian Zou
Huan Song
Zhimin Ma
Weinbin Hu
Electronic Information School,
Wuhan University,
Wuhan, Hubei 430072,
China

Huan Song
Electrical, Computer & Energy Engineering,
University of Colorado Boulder,
Boulder, CO 80309-0425,
USA

INTRODUCTION

During the sediment transport process, research on real-time measurements of sediment particles' incipient movement and suspended-load sediment concentration, including its spatial distribution, bed-load sediment motion and riverbed erosion and deposition, is of vital theoretical and practical significance (Roushangar *et al.* 2011; Foreman *et al.* 2013; Hazan *et al.* 2014; Liang *et al.* 2014; Zou *et al.* 2014; Xiao *et al.* 2015) At present, there is no feasible and reliable effective method to measure sediment incipient velocity during hydraulic model experiments (Liao *et al.* 2015). The measurement of suspended sediment concentration (SSC) and topography bedforms basically belong to point measurement, and it is impossible to directly obtain the real-time spatial distribution of SSC or the visualization and dynamic monitor of topography bedforms (such as a topographic bed made up of pulverized coals) (Guerrero *et al.* 2013; Nitsche *et al.* 2013; Apell & Gschwend 2016; Han *et al.* 2017). The real-time monitoring of bedform motion under the muddy water, including moving sediment particles near the riverbed, is also hard to achieve using

doi: 10.2166/hydro.2017.025

traditional optic or acoustic methods (Zou *et al.* 2014, 2015; Cristo *et al.* 2015; Ozger & Kabatas 2015). All of these issues have restricted the research of sediment movement law and the fast development of hydraulic model experiment measurement techniques.

Recently, ultrasound imaging detection has been developing fast, including traditional medical diagnosis, such as the B-mode ultrasound device. A B-mode ultrasound device is a kind of ultrasonic diagnostic apparatus, among which is the widely used medical diasonograph. It has a variety of operation modes according to different clinical diagnostic objectives. The B-mode of this device can be used to obtain a two-dimensional profile image of an observed target. The profile image obtained by the B-mode ultrasound device can reflect the inner outline of an object, which other acoustic methods and optical methods cannot do, especially when used in sediment-laden flow or muddy water. Sediment particles and the topographic bed are often clouded by moving or suspended particles. The profile image cannot be achieved by traditional optical/acoustic methods. Thus, using a B-mode ultrasound device to obtain the profile image is a better method, and can be further applied for the visual measurement of sediment-laden flow and underwater topographic riverbeds after image processing. According to phase-array ultrasonic imaging principle, an ultrasonic beam that is transmitted from a B-mode ultrasound device has good penetration in sediment-laden flow (Bamberger & Greenwood 2004; Pal & Ghoshal 2015). It can realize the real-time imaging of the sediment transport process. Therefore, this paper directly uses a B-mode ultrasound device to obtain the real-time imaging of sediment-laden flow and underwater topography. We obtained many B-mode ultrasound images of suspended-load particles, bed-load sediments and underwater topography, under clear or muddy water during our hydraulic model experiments.

From the obtained B-mode ultrasound images, the statistical analysis of suspended sediment particles' imaging spots, we can obtain the SSC and its spatial distribution in the water. Through the recognition and extraction of the topography bedform imaging bright band, we can achieve the real-time measurement and 3D reconstruction of the surface bed under muddy water. When the sediment particle source is fixed and flow condition is under control, we can obtain the incipient motion states of bed-load sediment particles under the effect of different water flows. After statistical analysis of the number of moving sand particles and the imaging boundary of the topographic surface at the same time, during multiple frame images, we can realize the measuring analysis of sediment incipient motion and incipient velocity. Therefore, ultrasound imaging measurement and real-time dynamic analysis of SSC, including its space distribution, flow velocity and field, sediment incipient velocity and underwater topographic bed during sediment transport process can be realized after suitable image processing. This will promote the development of sediment movement law and related hydraulic model experiment measurement techniques. Thus, for B-mode ultrasound imaging measurement issues of SSC, underwater topography, flow velocity field and sediment incipient velocity during sediment transport process in hydraulic model experiment, we put forward some novel solutions and measuring methods.

ULTRASOUND IMAGING SYSTEM

Imaging principle

As we all know, B-mode ultrasound diagnostic apparatus is widely used in medicine, and hearts and kidneys and even blood vessels are clearly shown by using this device (Zhou *et al.* 2013). The ultrasonic probe of the B-mode ultrasound diagnostic apparatus transmits a series of acoustic waves and receives the echoes of waves back from the human body. The frequency of acoustic wave is higher than 20 kHz (generally around 1–20 MHz) with strong penetrability after a series of echoes' signal processing inside the device. The ultrasonic probe is a kind of phased array probe based on piezo-electric effect, which can be controlled by humans according to the requirement of the imaging target. The ultrasound imaging of the human body can be realized after a series signal control and processing. The ultrasound imaging principle of a B-mode ultrasound device for sediment-laden flow in hydraulic model experiments is the same. The probe of the B-mode ultrasound device generates ultrasonic waves to water, and the ultrasonic waves are reflected from sediment or the topographic bed. Then, the probe receives their echoes. The time of passage of the ultrasonic waves is measured electronically and allows for the determination of the distance from sediments to the probe. Lastly, a profile image of the inner object is formed after a series of signal processing steps within the B-mode ultrasound device. Thus, the ultrasound images of sand or sediment in the water are formed in this way. The B-mode ultrasound device used is SIUI APOGEE 1100 Digital Color Doppler Ultrasound Imaging System, named APOGEE 1100 for short, and is shown in Figure 1.

When using a B-mode ultrasound device to obtain images of sediment-laden flow during sediment transport process in the water, a suitable configuration is important for later analysis and measurement. The B-mode ultrasound device has a linear array probe which can transmit 5 MHz, 10 MHz, and 12 MHz ultrasonic waves and a convex array probe which can transmit 2.0 MHz, 2.5 MHz, 3.3 MHz, 4.2 MHz, and 5.0 MHz ultrasonic waves. A frequency of 5 MHz was used in this paper. The other settings (e.g., TGC) were adjusted to obtain a good image before calibration and then remained the same when under different conditions in the case of unnecessary inner influence from the devices. There is little difference regarding particle imaging signals between different scanners under the same sediment situation when the settings are kept the same. In this paper, most experiments are performed by using the convex array probe. Because this device was originally used for medical diagnosis, its measuring depth is less than 40 cm and its measuring width is less than 38 cm. Its measuring angle is from 10° to 70°. The acquisition frame frequency ranges from 8 Hz to 63 Hz. It is worth noting that a number of TGC settings from the top to bottom remain the same during all experiments.

High frequency ultrasonic waves transmitted from the B-mode ultrasound device are sensitive to sediments or tiny particles underwater because of stronger penetrability when compared with traditional optical methods and single-beam ultrasonic methods (Smith *et al.* 1991; Leung *et al.* 2009; Pugh & McCave 2011; Gao *et al.* 2016; Yao *et al.* 2016). Suspended sediments can be monitored very well, especially with the help of modern B-mode ultrasound imaging technology. The B-mode ultrasound device can obtain the images of moving particles in sediment-laden flow. The imaging can follow the change of suspended sediments, just as shown in Figure 2, which is the profile map of

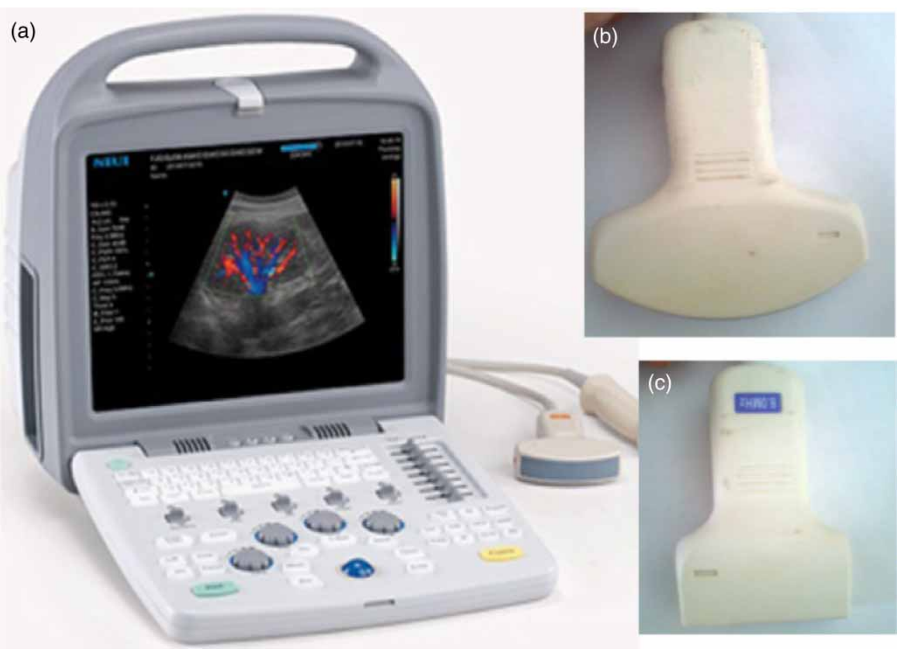

Figure 1 | B-mode ultrasound device: (a) the mainframe, (b) the convex probe, and (c) the linear probe.

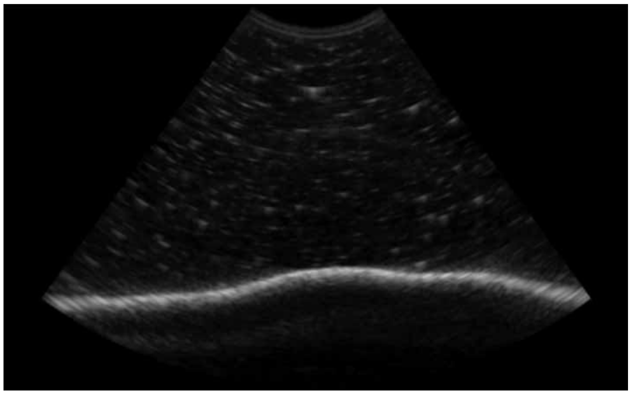

Figure 2 | B-mode ultrasound imaging of underwater sediments and topographic bed.

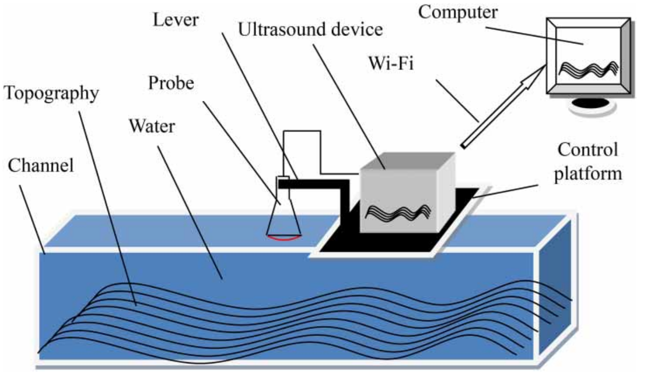

Figure 3 | An example of the application system.

sediment-laden flow including a riverbed under muddy water flow.

Figure 2 is the imaging of plastic sediments with particle size 0.32 mm and also the imaging of the topographic bed consisting of them. From Figure 2 it can be seen that the imaging of underwater suspended sediments and the topographic bed on the bottom is clear. The imaging spots of suspended sediments or moving particles are observed well with good self-adaption and high resolution.

Application system

To obtain video images of underwater model topography, an ultrasound imaging system for moving sediment particles and submerged topography acquisition is made up of an improved medical B-mode ultrasound device, a computer, a moving control system, and model topography in the water channel. The steady flow of a fluid in a long rigid tank is shown in Figures 3 and 4. A 5 Hz probe is connected to the B-mode ultrasound device, which is mounted at the water surface of a circulating water tank and enables a region of interest approximately $10 \times 35\ \mathrm{cm}^2$ from the probe to be monitored. The probe is fixed in line with the main flow axis in the tank, so the major movement of fluid is across the imaging sheet. A fixed voltage is supplied to the pump to introduce a steady flow rate over the time of measurement. The experiment system can generate a two-dimensional ultrasound image with an effective resolution of 640×480 pixels, where the spatial resolution is approximately 32×32 pixels per cm^2. The frame rate of the system is up to 60 frame/second. This is shown in Figure 3 and a photograph of the application system is shown in Figure 4.

Figure 4 | A photograph of the application system.

The size of the water channel in Figure 4 is $5.0\ \mathrm{m} \times 1.2\ \mathrm{m} \times 1.0\ \mathrm{m}$ (length × width × depth). The probe of the B-mode ultrasound device touches the water and collects the imaging signals of the underwater model topography. The collected imaging signals of water flow are sent to the computer, which analyzes the imaging signals and shows their processing results. The actual moving sediment particles and the submerged topographic beds are made up of model sands, such as plastic sand and natural sands which are widely used in hydraulic model experiments. This system shown in Figures 3 and 4 is used to demonstrate the application of the ultrasound imaging measurement method during a sediment transport process in the water channel.

IMAGING MEASUREMENT METHOD

Statistics of imaging spots

In order to count the number of suspended particles in the B-mode ultrasound image, a pixel labeling method based on the morphological risk estimation was used to identify the statistical sand spot. The flow chart of the method is shown in Figure 5. In order to make the method work better, this method takes a threshold segmentation method to analyze the imaging spots after a series of image preprocessing. When there is sandy terrain under the water during the experiment, due to the strong reflection of sandy terrain, the imaging bright band of underwater topography will cause a large white area at the lower part of the image, which causes in general higher pixel values at the bottom. When the SSC in the water is too high, due to excessive suspension above the water flow, which will cause a strong attenuation of the ultrasonic signals, the imaging spots in the upper part of the image are greater than the imaging spots in the lower part of the bright band. Therefore, the upper part of the image is generally brighter while the middle and bottom parts of the image are dim. Thus, the widely used global threshold and dynamic threshold method are not suitable for all cases of our sediment imaging spots' image, i.e., the B-mode ultrasound image will be applied for measuring and analyzing sediment imaging spots.

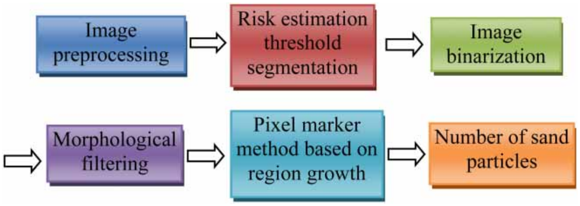

Figure 5 | Flow chart of recognition and statistical method for sediment imaging spots.

As shown in Figure 5, some preprocessing methods before the application of the ultrasound imaging measurement method are described as follows. For the statistical problems of suspended sediment particles' imaging spots in the B-mode ultrasound image, this paper proposes a pixel labeling method based on morphological risk estimates (Tsantis *et al.* 2009; Golemati *et al.* 2014). After image preprocessing, the method uses Bayesian risk estimation for sediment particle imaging spots and topographic imaging the bright band, and decides the threshold of minimum cost for image binarization threshold segmentation. Then, it adopts a morphological filtering method and a pixel labeling method based on regional growth to realize the statistical analysis of the number of sediment imaging spots (Shuster *et al.* 2014). This method can effectively solve the optimization problems of speckle noise and sediment imaging spots' adhesion or folding over the image. It realizes the imaging spots' statistical problem of suspended or moving sediment particles in the B-mode ultrasound image. For example, one of the processing results by using this method is shown in Figure 6. Figure 6(a) is the original ultrasound image and 115 spots counted by manual operation. Figure 6(b) is the statistical 330 spots after using Bayesian risk estimation. Figure 6(c) is the statistical 131 spots after using image binarization threshold segmentation. Figure 6(d) is the last statistical 114 spots after using a morphological filtering method and a pixel labeling method. Figure 6 well testifies the feasibility of the pixel labeling method based on morphological risk estimation.

Extraction of imaging bedform

In order to preserve the original information of the B-mode ultrasound image, such as the imaging signal of the suspended sediments at the top of the image, an adaptive tracking extraction method for the boundary of riverbed form is proposed based on the imaging bright band of topography. This method ignores the noise interference in the B-mode ultrasound image and only focuses on the imaging bright band region. Starting from the relatively strong central region of the imaging band, and scanning from top to bottom to obtain a point in the imaging band, the obtained

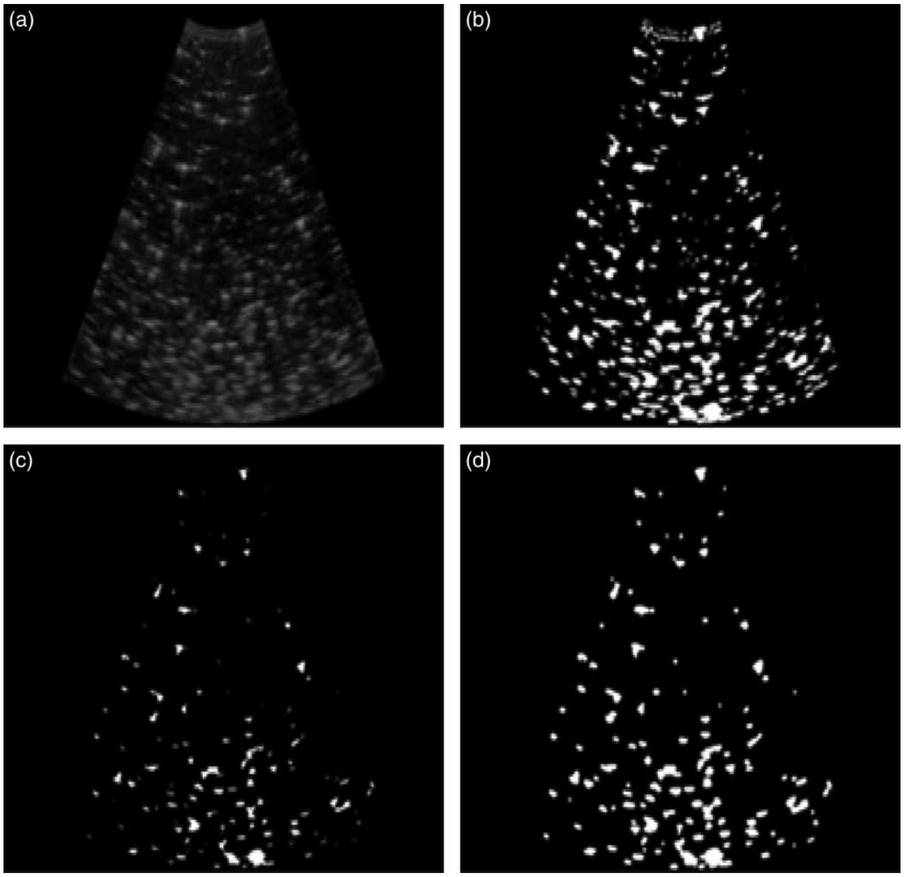

Figure 6 | Statistical results of sediment particles' imaging spots in B-mode ultrasound image: (a) the original ultrasound image and the 115 spots counted by manual operation; (b) the statistical 330 spots after using Bayesian risk estimation; (c) the statistical 131 spots after using image binarization threshold segmentation; (d) the last statistical 114 spots after using a morphological filtering method and a pixel labeling method.

point is taken as the starting point of the tracking process. Then both sides of the imaging band automatically track the boundary line. This method is self-adaptable and fast running, and can realize the single pixel extraction of the boundary line in the image. The flow chart of the adaptive tracking extraction method for the imaging boundary line of underwater topography bedform is shown in Figure 7.

In the case of sediment imaging spots, interference noise and gray gradient features of imaging the bedform, this method uses the sum of gray and gradient as the basis of judgment of the bedform boundary, that is, the position where the maximum value of the sum of the gradient and the grayscale can be taken as the bed topography boundary. Since the topography bedform is distributed along the horizontal direction,

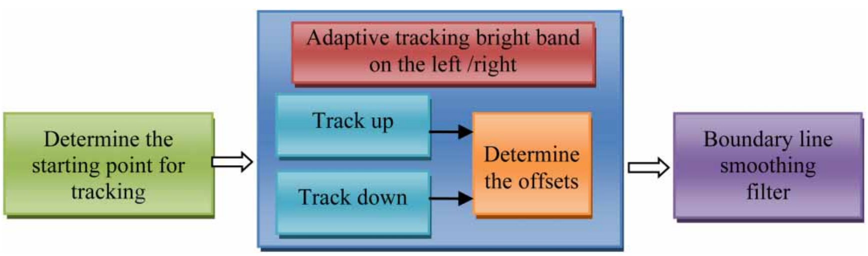

Figure 7 | The flow chart of the adaptive tracking extraction method for imaging bedform.

the extraction of the bedform boundary lines only takes the vertical gradient into account in practical engineering applications.

When using ultrasound imaging measurement method in the water channel during hydraulic model experiments, we can find the imaging of the topography bedform, e.g., Figure 2. For the identification and extraction of topographic bed's imaging bright band in the B-mode ultrasound image, this paper proposes the adaptive tracking extraction method for the imaging bright band of underwater bedform, and then uses an adaptive wavelet threshold denoising method based on contraction coefficients of wavelet domain. By using the imaging characteristics of the bed imaging bright band, the method ignores the interferences of the speckle noise and the other imaging spots, and just focuses on the imaging bright band of the topographic bed. Thus, the method starts from the center of the image where the imaging signal is relatively strong, and scans from up to down, and then obtains one point of imaging band as the starting point in tracking. Lastly, it scans out to two sides of the starting point for automatic tracking of the imaging bright band. This method is fast, and has the advantage of strong adaptability. It implements the one-pixel-wide extraction of the topographic boundary at once. This method solves the real-time monitoring and online analysis of topographic beds under complex or muddy water flow conditions. Some results of extracted imaging bands for underwater topography bedforms are used as examples and shown in Figure 8.

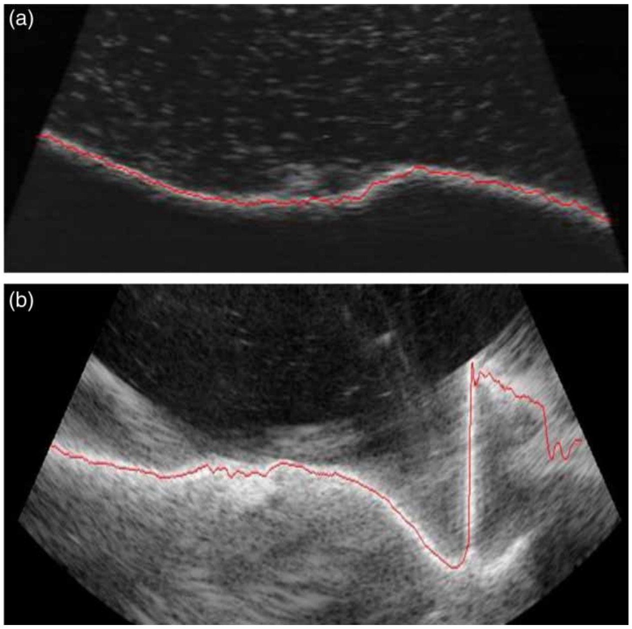

Figure 8 | The adaptive tracking extraction results of the imaging bright band for topographic riverbed under the water flow: (a) the bedform consists of plastic sand and (b) an unnaturally changed topography consists of natural sands and cobblestones with a vertical barrier above the bottom.

Measurement of imaging particle velocity

In order to measure the moving velocity of imaging spots in the ultrasound image, we take an ultrasound particle image velocimetry (UPIV) method based on the velocimetry algorithm and the sweep correction. Just like optical particle image velocimetry (PIV) analysis, this UPIV method is also based on a cross-correlation technique, such as Figure 9.

Because the number of pixels in a UPIV image is generally smaller than in an optical PIV image, advanced techniques for increasing spatial resolution are essential. Thus, an improved method that brings enhancement in accuracy for the examination of UPIV images is described in this paper (Wang & Zheng 2008). This method is based on cross-correlation with discrete window offset (Sugii *et al.* 2000), which makes full use of a translation of the second interrogation window deformation and rebuilds it considering the rotation and shear. The displacement extracted from UPIV images is predicted and corrected by means of an iterative procedure. The flow chart of the UPIV method is shown in Figure 10.

We take a multi-grid interrogation algorithm by using a hierarchical approach. Then the particle image displacement is measured by cross-correlation function under an assumption that the motion of the particles' image within the interrogation window is almost uniform. Due to the varying displacement field, the image intensity has to be interpolated at non-integer pixel location which will increase the computational load. Multi-step analysis of UPIV images can be viewed as comprising two procedures: multi-grid analysis and iterative analysis.

The fundamental difference between optical PIV and UPIV is the timing of the image formation. In optical PIV, a CCD device obtains a snapshot of the tracer images. In UPIV, the image is constructed by sequentially recording scan lines. This means that different parts of the ultrasound image are recorded at different times, while in optical PIV the velocity is yielded simply by dividing the displacement

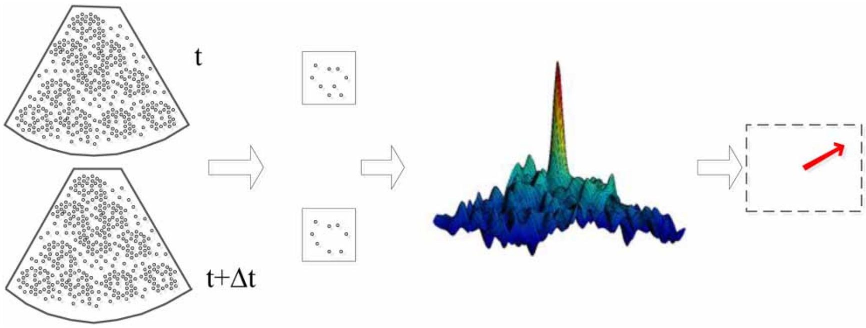

Figure 9 | Principle of the UPIV process.

by the time interval between frames. In UPIV, the time interval is actually also a function of the displacement.

APPLICATION RESULTS AND DISCUSSION

This section describes several kinds of applications of B-mode ultrasound imaging measurement method based on the above-described methods during the sediment transport process in the water channel of the physical model experiment shown in Figures 3 and 4. The applications in measuring SSC, topography bedform, moving particle velocity or flow field and sediment incipient velocity are described as follows. We provide some examples to show these applications and discuss their actual application results.

SSC measurement

According to the section 'Statistics of imaging spots' and the pixel labeling method based on morphological risk estimation, we further statistically analyze the imaging area concentration of all counted imaging spots after using the pixel labeling method to count the number of imaging particles in the B-mode ultrasound image. We used a calibration test for the statistical analysis of the relationship between imaging area concentration and suspended sediment in the water flow. The calibration test result is shown in Table 1. The statistical data of Table 1 show the relationship is relatively stable and clear.

According to the relationship between sediment imaging spots and SSCs in the water flow, this paper describes a method to measure SSC and its spatial distribution based on the B-mode ultrasound imaging method. By analyzing the statistics of imaging area concentrations under different SSCs in the water flow, the relationships between these statistical concentrations are established by a further calibration test. According to the calibration test and the relationship in Table 1, the imaging measurement of unknown SSC can be realized in the sediment-laden flow. Meanwhile, according

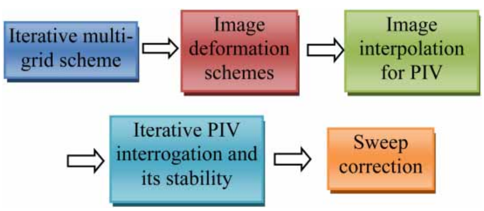

Figure 10 | The flow chart of recognition and statistical method for sediment imaging spots.

Table 1 | The relationship between the imaging area concentration (counted imaging spots/all spots in the image) and actual SSC during the calibration test

Suspended sediment concentration/%	Imaging area concentration/%
0.00	0.02
0.05	28.9
0.10	55.1
0.15	74.2
0.20	86.8
0.25	91.5
0.30	94.1
0.35	95.2
0.40	96.1
0.45	96.9
0.50	97.7

to the position distribution of suspended particles' imaging spots in the image, the spatial distribution analysis and hierarchical measurement along with the depth of sediment concentration also can be realized. Calibration tests show this method can be suitable for the imaging measurement of SSC with less than 0.5% or about 10 kg/m^3 at present. This method has high sensitivity, is good in real time, and can monitor water flow without human disturbance. B-mode ultrasound imaging can measure in real time the dynamic changes of SSC and its space distribution in sediment-laden flow. This novel application example of measuring sediment concentration is shown in Figure 11.

Topography bedform measurement and reconstruction

For the real-time monitoring and visualization analysis problems of topography bedforms under muddy water, the visualization measurement and reconstruction of underwater topography bedforms can be realized by using the adaptive tracking extraction method described in the section 'Extraction of imaging bedform'. Based on the similarity and gradual change of topographies in consecutive frames, the method can automatically track topographic lines of riverbed imaging bright band, and real-time monitor the change of bed boundary, and then use the tracked boundary lines to reconstruct the original 3D topography bedform surface. The measurement and 3D reconstruction example of underwater topography is shown in Figure 12.

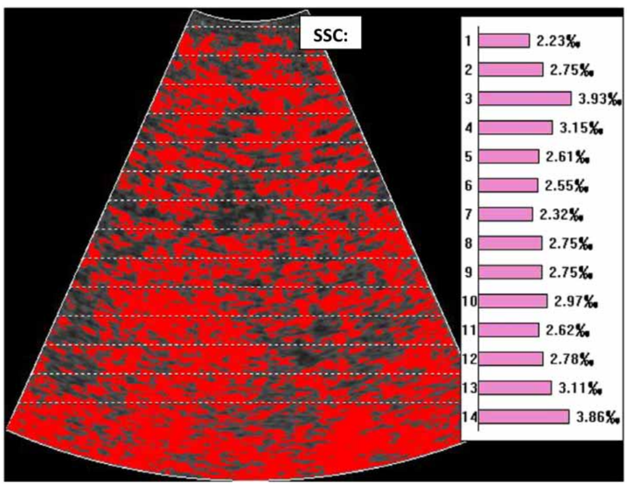

Figure 11 | The measurement application of SSC and the analysis of its space distribution in sediment-laden flow.

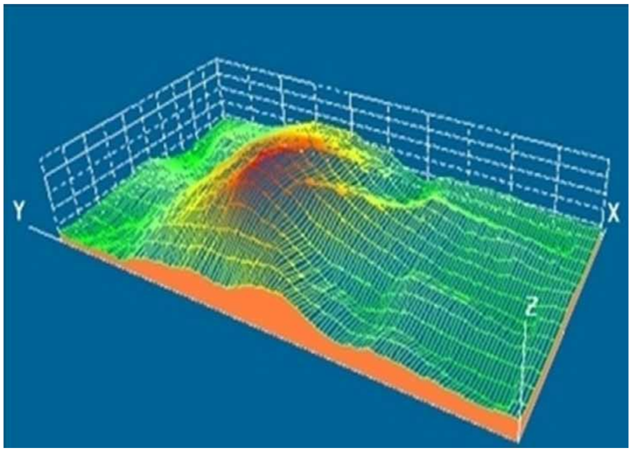

Figure 12 | The measurement and 3D reconstruction of underwater topography bedform.

In order to illustrate the precision and repeatability of this B-mode ultrasound imaging measurement method against topographic bed truth values, we used the device to measure underwater topography and compared it with ultrasound single-beam system. They are conducted at the same fixed topographic bed at a relatively low SSC. Figure 13(a), 13(c) and 13(e) are under the condition of flow velocity 5.36 cm/s and SSC 0.386‰. Figure 13(b), 13(d) and 13(f) are under the condition of flow velocity 12.47 cm/s and SSC 0.517‰. The results of the comparison are shown in Figure 13 and discussed below.

Sediments in the water can deposit on the topographic bed surface and cover the fixed riverbed. From Figure 13, ultrasound imaging method (Y2) of this device and ultrasound single-beam system (Y1) can be used to detect underwater topography under a relatively low SSC and small flow velocity. When flow velocity is high enough for the movement of particles near the bed, the topographic boundary will be changed. The detection of the topographic bed will generate a big deviation. When flow velocity is 5.36 cm/s and SSC is 0.386‰, the deviation between ultrasound imaging (Y2) method and fixed line (Y3) of the riverbed is within 2 mm, and the deviation between single-beam system (Y1) and the fixed line (Y3) is within 3 mm. When flow velocity is 12.47 cm/s and SSC is 0.517‰, the deviation of Y2–Y3 is within 7 mm, and the deviation of Y1–Y3 is within 13 mm. The biggest deviation is at the position of 165 mm in Figure 13(b). These deviations have also included the thickness of sedimentary particles on the

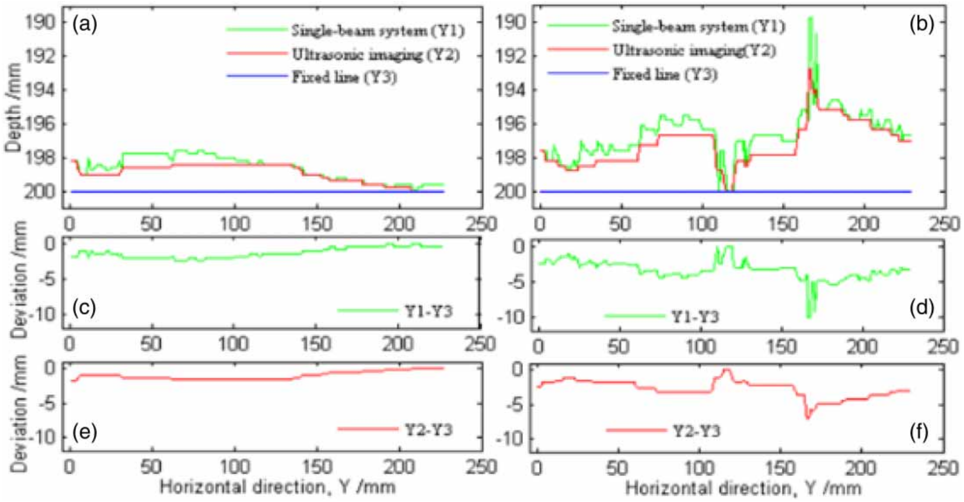

Figure 13 | Topographic bed measurement under muddy water: (a) and (b) are the fixed lines (Y3) of the topographic bed in comparison with ultrasound imaging (Y2) method by using B-mode ultrasonic device and ultrasonic single-beam system (Y1); (c) and (d) are the deviations of Y1 and Y3; (e) and (f) are the deviations of Y2 and Y3; (a), (c) and (e) are under flow velocity 5.36 cm/s and SSC 0.386‰; (b), (d) and (f) are under flow velocity 12.47 cm/s and SSC 0.517‰.

riverbed. The sedimentary particles have formed a layer which is moving along the topographic bed. This is the main reason for a big deviation.

The comparison in Figure 13 shows that the visualization measurement and 3D reconstruction errors are not bigger than 1 mm for the topographic bed. This effectively eliminates the influence of moving particles, and recreates the original bedform under muddy water flow. Therefore, this method realizes the real-time dynamic measurement of the topographic bed and the statistical analysis of the topographic peak, trough, wavelength and its moving speed in the sediment-laden water flow. It provides an effective way to observe bedform sediment motion and the analysis of underwater topography bedform during hydraulic model experiments.

Moving particle velocity and flow field measurement

According to the section 'Measurement of imaging particle velocity', we can measure the velocity of moving particles in the water flow by using the UPIV method, which is based on the velocimetry algorithm and the sweep correction. Then we can obtain the flow field by measuring particles' imaging spots in the image. For example, two successive B-mode ultrasound images are used to measure the flow velocity of moving particles and the flow field in the water flow. Figure 14 shows two successive B-mode ultrasound images.

For the analysis, the two ultrasound images (Figure 14) are sub-divided into 64×64 pixel non-overlapping

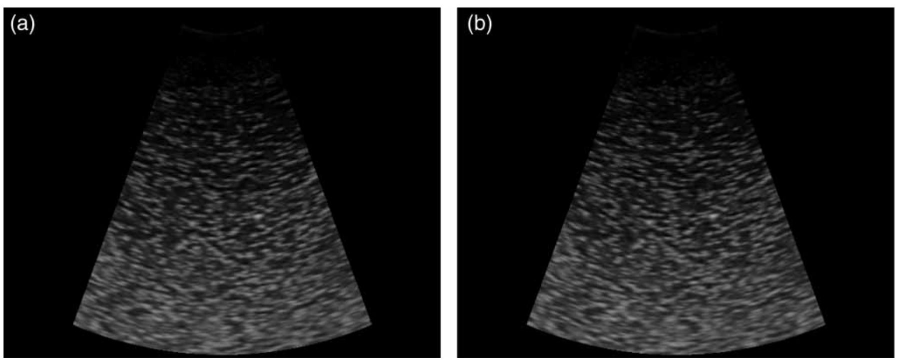

Figure 14 | Two B-mod two-dimensional ultrasound images at t and $t + \Delta t$.

interrogation images, with a shift of 16 pixels between successive interrogations. The corresponding sub-images are analyzed by the cross-correlation algorithm based on FFT. Figure 15 shows the instantaneous depth-averaged velocity vector results for sediment-laden flow.

Actually, the flow field is not reproducible, but we have to compare the measured result, yield at different times. The basic strategy in such a situation is to replace the instantaneous velocities by corresponding ensemble averages. The other assumption is that the random field is ergodic with respect to the mean and covariance. The statistics of depth-averaged velocity is derived by 50 sequential UPIV images. Depth-averaged velocity statistics are obtained from the UPIV velocity fields by averaging data along the vertical direction of constant in each field, and then ensemble averaging the line averages over the full set of 50 fields. Meanwhile, after a serial experiment in steady flow condition, the actual depth-averaged vertical distribution has also been obtained by acoustic Doppler current profiler (ADCP) method, which can be regarded as the standard velocity. The best way to verify that the depth-averaged velocity vectors are valid would have been comparison of the standard velocity at several locations, so the results are compared with the measurement results by using the ADCP method.

In order to assess the validation for estimating local depth-averaged velocities, first, it gets a value using all measurements at each sampling position, and assumes that represents a true value. Second, the depth averaged velocity distribution of the sediment-laden flow is chosen as the statistic compared with the standard velocity obtained by the ADCP method. The depth-averaged velocity distribution of the sediment-laden flow is obtained by ensemble averages and is listed among 50 ultrasound PIV images in Table 2.

Figure 15 and Table 2 show the different ensemble averaged velocity profiles in the water flow. Profiles of depth-average velocity are logarithmic in form and exhibit the strong influence of form drag associated with coarse bed roughness. The logarithmic profiles are approximately valid over the entire flow depth. The profile flow field obtained by the ADCP method has significant agreement with theoretical value, which is a Doppler measurement technique that has been verified. One interesting observation that can be drawn is that the velocity profile of the UPIV method is lower than the actual velocity. In fact, the profile flow velocity obtained by UPIV has a much better agreement with actual velocity during hydraulic model experiments after comparison with some other data, which are obtained by laser Doppler velocimetry and propeller type current meter.

Sediment incipient velocity measurement

As the boundary of underwater topography surface can be obtained by continuous trace extraction, and the flow velocity of moving particles in the water can be measured by

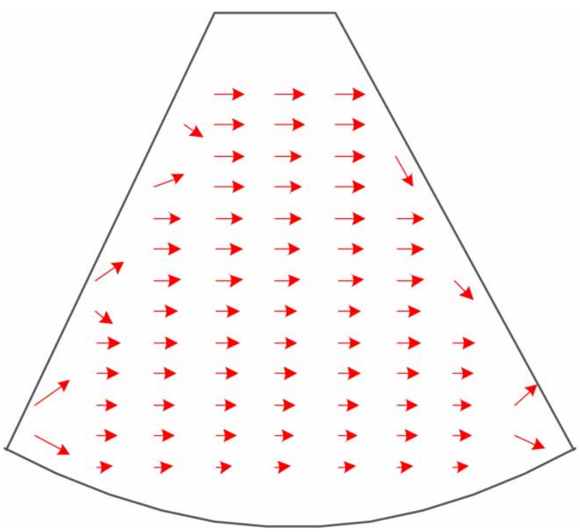

Figure 15 | The raw vector map obtained by the UPIV method.

Table 2 | The depth-averaged velocity distributions of the sediment-laden flow obtained by the ADCP method and the UPIV method

	Velocity (cm/s)	
Depth (cm)	**ADCP method**	**UPIV method**
2.5	11.02	10.82
5.0	10.99	10.69
7.5	10.94	10.64
10.0	10.93	10.72
12.5	10.82	10.52
15.0	10.77	10.47
17.5	10.66	10.36
20.0	10.49	10.35
22.5	10.38	10.08
25.0	10.17	9.87
27.5	10.02	9.82

using the UPIV method, we can monitor the sediment incipient motion near the surface bed and then obtain the incipient velocity of sediment particles. From the above, the imaging spot number in the image can be counted according to the described method of the section 'Statistics of imaging spots'. The imaging boundary of the underwater topographic bed in the image can be tracked automatically and reconstructed according to the described method of the section 'Extraction of imaging bedform'. The flow velocity of moving particles near the topographic bed can also be measured according to the described method of the section 'Measurements of imaging particle velocity'. Therefore, analysis of sediment incipient motion and the measurement of sediment incipient velocity can be realized by using the above-described methods in the section 'Imaging measurement method'.

After different kinds of model experiments, results show there are the same features in the image for the imaging signals of different sand materials and particle sizes, that is, the imaging spot number of sand particles near the bed is low when flow velocity is smaller than sediment incipient velocity, and the imaging spot number increases slowly with the increase of the flow velocity. However, the imaging spot number is suddenly increased when the flow velocity is up to or bigger than the sediment incipient velocity, and the related curve of the imaging spot number changes hugely. According to these features, through multiple sets of water channel experiments with different flow sections, the imaging spot number curves changing with flow velocities are obtained, and their change rate curves are also analyzed. The extreme turning points of these curves are analyzed when the sand imaging spots are suddenly changed. The imaging sediment particle undergoes a mutation process during the sediment incipient process. According to the mutation process, the sediment incipient movement is determined and its incipient velocity can be measured based on the corresponding flow velocity (Zou *et al.* 2017). Lastly, the measured sediment incipient velocities are verified by using the measured topographic bed and the UPIV method. An example of measuring sediment incipient velocity is shown in Figure 16.

According to the sudden addition phenomenon of imaging particle spots near the bed surface in the B-mode ultrasound image, the sediment incipient velocity can be measured by using the counted imaging spot number, the obtained topographic bed, and the UPIV method. The measuring principle is in accordance with the sediment incipient motion and related principles, and the measured sediment incipient velocity can be verified by the UPIV method during the water channel experiments.

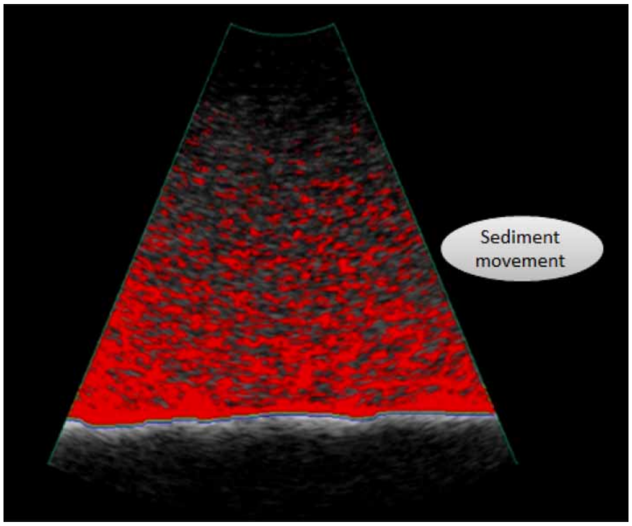

Figure 16 | Monitoring and analysis of sediment particles' movement and the changed riverbed during the sediment transport process.

CONCLUSIONS

This paper proposes a B-mode ultrasound imaging measurement method and its application system, and then realizes the visualization measurement of sediment particles, underwater topographic bed and flow velocity by using this system under muddy water or in sediment-laden flow. Further applications of this ultrasound imaging method and system have also realized sediment-laden flow imaging measurements of the main motion features during the sediment transport process in hydraulic model experiments. These applications are about the real-time measurements of SSCs including their space distribution, topography bedform and flow field and sediment incipient velocity near the riverbed surface. These water-flow parameters are vital for the whole sediment transport process during hydraulic model experiments. This is of vital significance for the research of water–sand interaction mechanism, sediment transport law, and riverbed evolution law. Another B-mode ultrasound imaging method has realized the visual measurements of sediment-laden flow and motion process of bedform sediments. It brings traditional complex point measurement research into intuitive and fast image measurement research with linear, square, and cubic styles. Using the B-mode ultrasound imaging measurement method paves a novel approach for the measurement problems of muddy water or sediment-laden flow during hydraulic model experiments.

ACKNOWLEDGEMENTS

Some figures and data in this paper are based on unpublished data obtained during earlier studies in collaboration with Prof. Zhimin Ma and Dr Wenbin Hu, and some figures and partial data are from my unpublished doctoral dissertation at the Electronic Information School, Wuhan University. The authors acknowledge Dr Wenbin Hu's contributions in acquiring the data and the fruitful discussions about ultrasound techniques. The authors and their affiliation gratefully acknowledge the permissions granted to reproduce the copyright material in this review. This paper was supported by the National Natural Science Foundation of China (Grant No. 41402278 and Grant No. 41372317).

REFERENCES

Apell, J. N. & Gschwend, P. M. 2016 In situ passive sampling of sediments in the Lower Duwamish Waterway Superfund site: replicability, comparison with ex situ measurements, and use of data. *Environmental Pollution* **218**, 95–101.

Bamberger, J. A. & Greenwood, M. S. 2004 Using ultrasonic attenuation to monitor slurry mixing in real time. *Ultrasonics* **42** (1), 145–148.

Cristo, C. D., Greco, M., Iervolino, M., Leopardi, A. & Vacca, A. 2015 Two-dimensional two-phase depth-integrated model for transients over mobile bed. *Journal of Hydraulic Engineering* **142** (2), 04015043.

Foreman, M. R., Giusca, C. L., Coupland, J. M., Török, P. & Leach, R. K. 2013 Determination of the transfer function for optical surface topography measuring instruments – a review. *Measurement Science and Technology* **24** (5), 052001.

Gao, Y., Liang, T., Tian, S., Wang, L., Holm, P. E. & Bruun Hansen, H. C. 2016 High-resolution imaging of labile phosphorus and its relationship with iron redox state in lake sediments. *Environmental Pollution* **219**, 466–474.

Golemati, S., Lehareas, S., Tsiaparas, N., Gastounioti, A., Chatziioannou, A., Nikita, K. & Perrea, D. 2014 Toward recognizing the vulnerable asymptomatic atheromatous plaque from B-mode ultrasound: the importance of the morphology of the plaque shoulder. In: *IEEE International Ultrasonics Symposium*, 3–6 September, Chicago, IL, pp. 2390–2393.

Guerrero, M., Di Federico, V. & Lamberti, A. 2013 Calibration of a 2-D morphodynamic model using water-sediment flux maps derived from an ADCP recording. *Journal of Hydroinformatics* **15** (3), 813–828.

Han, C., Ren, J., Wang, Z., Tang, H. & Xu, D. 2017 A novel hybrid sensor for combined imaging of dissolved oxygen and labile phosphorus flux in sediment and water. *Water Research* **108**, 179–188.

Hazan, Y., Wangensteen, O. S. & Fine, M. 2014 Tough as a rock-boring urchin: adult *Echinometra* sp. EE from the Red Sea show high resistance to ocean acidification over long-term exposures. *Marine Biology* **161** (11), 2531–2545.

Leung, H., Schindler, K., Chan, A. Y., Lau, A. Y., Leung, K. L., Ng, E. H. S. & Wong, K. S. 2009 Wavelet-denoising of electroencephalogram and the absolute slope method: a new tool to improve electroencephalographic localization and lateralization. *Clinical Neurophysiology* **120** (7), 1273–1281.

Liang, D., Zeckoski, R. W. & Wang, X. 2014 Development of a hydro-environmental model for inland navigational canals. *Journal of Hydroinformatics* **16** (3), 572–587.

Liao, Q., Wang, B. & Wang, P.-F. 2015 In situ measurement of sediment resuspension caused by propeller wash with an underwater particle image velocimetry and an acoustic Doppler velocimeter. *Flow Measurement and Instrumentation* **41**, 1–9.

Nitsche, M., Turowski, J. M., Badoux, A., Rickenmann, D., Kohoutek, T. K., Pauli, M. & Kirchner, J. W. 2013 Range imaging: a new method for high-resolution topographic measurements in small- and medium-scale field sites. *Earth Surface Processes and Landforms* **38** (8), 810–825.

Ozger, M. & Kabatas, M. B. 2015 Sediment load prediction by combined fuzzy logic-wavelet method. *Journal of Hydroinformatics* **17** (6), 930–942.

Pal, D. & Ghoshal, K. 2015 Grain-size distribution in open channel flow by mixing length approach. *Environmetrics* **26** (2), 107–119.

Pugh, R. S. & McCave, I. N. 2011 Particle size measurement of diatoms with inference of their properties: comparison of three techniques. *Journal of Sedimentary Research* **81** (8), 600–610.

Roushangar, K., Hassanzadeh, Y., Keynejad, M. A., Alami, M. T., Nourani, V. & Mouaze, D. 2011 Studying of flow model and bed load transport in a coarse bed river: case study – Aland River, Iran. *Journal of Hydroinformatics* **13** (4), 850–866.

Shuster, A. K. G., Fischer, J. E. & Vossmerbaeumer, U. 2014 Semi-automated retinal vessel analysis in nonmydriatic fundus photography. *Acta Ophthalmologica* **92** (1), e42–e49.

Smith, S. W., Pavy, H. G. & von Ramm, O. T. 1991 High-speed ultrasound volumetric imaging system. I. Transducer design and beam steering. *IEEE Transactions on Ultrasonics, Ferroelectrics, and Frequency Control* **38** (2), 100–108.

Sugii, Y., Nishio, S., Okuno, T. & Okamoto, K. 2000 A highly accurate iterative PIV technique using a gradient method. *Measurement Science and Technology* **11** (12), 1666–1673.

Tsantis, S., Dimitropoulos, N., Cavouras, D. & Nikiforidis, G. 2009 Morphological and wavelet features towards sonographic thyroid nodules evaluation. *Computerized Medical Imaging and Graphics* **33** (2), 91–99.

Wang, J. & Zheng, H. R. 2008 A new velocimetry algorithm for optimizing ultrasonic PIV imaging method. In: *International Conference on Information Technology and Applications in Biomedicine*, 30–31 May, Shenzhen, China.

Xiao, X., Guo, B., Li, D., Zou, X., Zhang, P., Liu, J. C. & Zang, Y. F. 2015 Ultrasound imaging measurement of submerged topography in the muddy water physical model. *Measurement Science and Technology* **26** (8), 085304.

Yao, Y., Wang, P., Wang, C., Hou, J., Miao, L., Yuan, Y., Wang, T. & Liu, C. 2016 Assessment of mobilization of labile phosphorus and iron across sediment-water interface in a shallow lake (Hongze) based on in situ high-resolution measurement. *Environmental Pollution* **219**, 873–882.

Zhou, B., Fraser, K. H., Poelma, C., Mari, J.-M., Eckersley, R. J., Weinberg, P. D. & Tang, M.-X. 2013 Ultrasound imaging velocimetry: effect of beam sweeping on velocity estimation. *Ultrasound in Medicine & Biology* **39** (9), 1672–1681.

Zou, X., Ma, Z., Zhao, X., Hu, X. & Tao, W. 2014 B-scan ultrasound imaging measurement of suspended sediment concentration and its vertical distribution. *Measurement Science and Technology* **25** (11), 115303.

Zou, X., Ma, Z., Hu, W., Wang, J., Song, H., Hu, X. & Tao, W. 2015 B-mode ultrasound imaging measurement and 3D reconstruction of submerged topography in sediment-laden flow. *Measurement* **72**, 20–31.

Zou, X., Wang, C., Song, H., Han, Z. & Ma, Z. 2017 Experimental measurements of sediment incipient velocity by using B-scan ultrasound imaging device in the water channel. *Measurement* **98**, 228–236.

First received 12 February 2017; accepted in revised form 16 November 2017. Available online 4 December 2017